

## Construction of 3D Layer-Pillared Homoligand Coordination Polymers from a 2D Layered Precursor

Jinyu Sun,<sup>†,§,\*</sup> Yaming Zhou,<sup>‡</sup> Qianrong Fang,<sup>§</sup> Zhenxia Chen,<sup>‡</sup> Linhong Weng,<sup>‡</sup> Guangshan Zhu,<sup>§</sup> Shilun Qiu,<sup>\*,§</sup> and Dongyuan Zhao<sup>\*,‡</sup>

Department of Chemistry, Fudan University, Shanghai 200433, P. R. China, and State Key Lab of Inorganic Synthesis & Preparative Chemistry, Jilin University, Changchun 130012, P. R. China

Received July 4, 2006

Herein, we present a new method for preparing homoligand 3D coordination polymers. First, a layered metal–organic framework  $Zn_3(BDC)_3(H_2O)_2 \cdot 4DMF$  **1** (BDC is terephthalate, DMF is *N,N*-dimethylformamide) was fabricated from a  $H_2BDC$  by liquid–liquid diffusion. Second, the layered product, **1**, was used as a precursor to solvothermally react with further  $H_2BDC$  at 140–180 °C, resulting in two products of BDC insertion into the layered structure. These are  $[Zn_3(\mu_4-BDC)_4] \cdot 2HPIP$ , **2** (HPIP is partly protonated piperazine), and  $[Zn_3(\mu_2-BDC)_3(H_2BDC)] \cdot (C_6H_{15}NO) \cdot H_2O \cdot 3DMF$ , **3** ( $C_6H_{15}NO$  is triethylamine *N*-oxide). Single-crystal X-ray diffraction shows that **2** possesses a layer-pillared structure of  $\mu_4$ -BDC, with 1D channels, while **3** has a layer-pillared structure of  $\mu_2$ -BDC, with 2D channels.  $N_2$ -sorption experiments show **3** has a relatively high BET surface area of 750 m<sup>2</sup>/g. It is proposed that **2** follows the crystal growth mechanism of Ostwald ripening, whereas the crystal structure of **3** might be formed by an insertion mechanism.

### Introduction

One-step self-assembly is one of the few practical strategies for the syntheses of molecular functional materials, particularly metal–organic frameworks (MOFs).<sup>1,2</sup> Many three-dimensional (3D) MOFs have been prepared by this strategy.<sup>3–6</sup> Particular attention has been given to some 3D MOF coordination polymers with high surface areas because

of their potential applications as absorbents, catalysts, and sensors.<sup>7,8</sup> However, products in this one-step process are unpredictable even if factors such as pH, counterion, solvent, metal ion, and ligand are controlled. Typically, 1D or 2D coordination polymers, such as MOF-2 and MOF-3,<sup>9–12</sup> are often formed as undesirable byproducts in our experiments. The layer-pillared 3D frameworks exhibit exceptionally high sorption capacity in comparison with 1D or 2D dynamic porous coordination polymers,<sup>13–24</sup> so they have successfully been synthesized from substrates of metal–carboxylate sheets and organic amines or the reverse.<sup>15,16</sup> Until now, there have

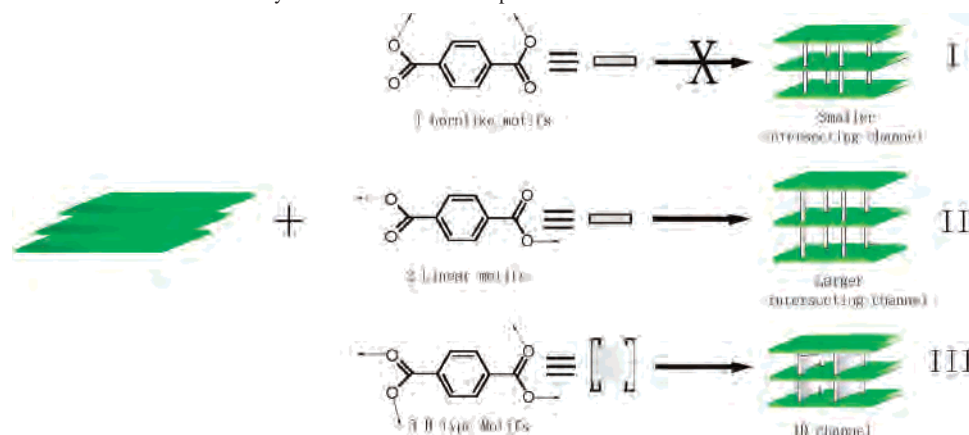
\* To whom correspondence should be addressed. E-mail: jinyusun@jlu.edu.cn (J.S.); dyzhao@fudan.edu.cn (D.Z.); slqiu@mail.jlu.edu.cn (S.Q.). Phone: 86-431-5168556. Fax: 86-431-5168331.

<sup>†</sup> Fudan University.

<sup>‡</sup> Jilin University.

- (1) (a) Whitesides, G. M.; Grzybowski, B. *Science* **2002**, *295*, 2418. (b) Cox, J. K.; Eisenberg, A.; Lennox, R. B. *Curr. Opin. Colloid Interface Sci.* **1999**, *4*, 52.
- (2) Rouvray, D. *Chem. Br.* **2000**, 26.
- (3) Hoskins, B. F.; Robson, R. *J. Am. Chem. Soc.* **1989**, *111*, 5962.
- (4) (a) Carlucci, L.; Ciani, G.; Proserpio, D. M.; Sironi, A. *Angew. Chem., Int. Ed. Engl.* **1995**, *34*, 1895. (b) Batten, S. R.; Houskins, B. F.; Robson, R. *J. Chem. Soc., Chem. Commun.* **1991**, 445. (c) Gable, R. W.; Houskins, B. F.; Robson, R. *J. Chem. Soc., Chem. Commun.* **1990**, 762. (d) Chen, B.; Eddaoudi, M.; Reineke, T. M.; Kampf, J. W.; O’Keeffe, M.; Yaghi, O. M. *J. Am. Chem. Soc.* **2000**, *122*, 11559. (e) Keller, S. W. *Angew. Chem., Int. Ed. Engl.* **1997**, *36*, 247. (f) Sun, J.; Weng, L.; Zhou, Y.; Chen, J.; Chen, Z.; Liu, Z.; Zhao, D. *Angew. Chem., Int. Ed.* **2002**, *41*, 4471. (g) Yaghi, O. M.; Davis, C. E.; Li, G.; Li, H. *J. Am. Chem. Soc.* **1997**, *119*, 2861. (h) Kerpet, C. J.; Prior, T. J.; Rosseinsky, M. J. *J. Am. Chem. Soc.* **2000**, *119*, 2861. (i) Chen, B.; Eddaoudi, M.; Hyde, S. T.; O’Keeffe, M.; Yaghi, O. M. *Science* **2001**, *291*, 1021. (j) Chui, S.; Lo, S.; Charmant, J. P. H.; Orpen, A. G.; Williams, I. D. *Science* **1999**, *283*, 1148.

- (5) Abrahams, B. F.; Haywood, M. G.; Robson, R.; Slizys, D. A. *Angew. Chem., Int. Ed.* **2003**, *42*, 1112.
- (6) Feréy, G.; Serre, C.; Draznieks, C. M.; Millange, F.; Surble, S.; Dutour, J.; Margiolaki I. *Angew. Chem., Int. Ed.* **2004**, *43*, 6296.
- (7) For reviews, see: (a) Rowsell, J. L. C.; Yaghi, O. M. *Micropor. Mesopor. Mater.* **2004**, *73*, 3. (b) Yaghi, O. M.; O’Keeffe, M.; Ockwig, N. W.; Chae, H. K.; Eddaoudi, M.; Kim, J. *Nature* **2003**, *423*, 705. (c) Rao, C. N. R.; Natarajan, S.; Vaidyanathan, R. *Angew. Chem., Int. Ed.* **2004**, *43*, 1466. (d) Kitagawa, S.; Kawata, S. *Coord. Chem. Rev.* **2002**, *224*, 11. (e) Eddaoudi, M.; Moler, D. B.; Li, H.; Chen, B.; Reineke, T. M.; O’Keeffe, M.; Yaghi, O. M. *Acc. Chem. Res.* **2001**, *34*, 319. (f) Moulton, B.; Zaworotko, M. J. *Chem. Rev.* **2001**, *101*, 1629. (g) Zheng, S. L.; Tong, M. L.; Chen, X. M. *Coord. Chem. Rev.* **2003**, *246*, 185. (h) Murray, K. S.; Kepert, C. J. In *Spin Crossover in Transition Metal Compounds I*; Topics in Current Chemistry Series 233; Springer-Verlag: Berlin, 2004; p 195. (i) Evans, O. R.; Lin W. *Acc. Chem. Res.* **2002**, *35*, 511. (j) Batten, S. R.; Robson, R. *Angew. Chem., Int. Ed. Engl.* **1998**, *37*, 1460.

**Scheme 1** Coordination Mode of BDC and the Layer-Pillared Structures Expected

been no reports of an open 3D homoligand coordination polymer prepared from 2D layered precursors. Below, we describe the methods to construct 3D layer-pillared homoligand coordination polymers by reassembling a BDC acid with its layered coordination polymer. Compound **1** is an example of a layered metal–BDC coordination polymer that can be prepared in good yield and then reacted with its BDC ligand, acting as a pillar, to create a 3D layer-pillared porous phase, as shown in Scheme 1. The scheme shows that BDC ligands are more successful in creating 3D pillared structures than the organic amines in the other reports. This scheme may also be useful in the synthesis of specific products and the investigation of the self-assembly mechanism of layer-pillared

coordination polymers, including whether layered intermediates are necessary precursors to layer-pillared structures.

Solvothermal treatment is an established method for secondary assembly of MOF coordination polymers,<sup>15,16</sup> and for pillaring of the layered clays.<sup>17</sup> In this paper, we describe the preparation of two 3D layer-pillared coordination polymers  $[\text{Zn}_3(\text{BDC})_4] \cdot 2\text{HPIP}$ , **2**, and  $[\text{Zn}_3(\text{BDC})_3(\text{H}_2\text{BDC})] \cdot (\text{C}_6\text{H}_{15}\text{NO}) \cdot \text{H}_2\text{O} \cdot 3\text{DMF}$ , **3**, by secondary solvothermal processes in good yields from the layered precursor **1**. All the products were characterized by powder X-ray diffraction (PXRD), single-crystal X-ray diffraction (SCXRD), and thermogravimetric analysis (TGA).  $\text{N}_2$  sorption and the crystal growth mechanism have also been studied.

## Experimental Section

**General Methods and Materials.** All the chemical reagents were obtained commercially (Aldrich) and were used without further purification. The PXRD patterns were obtained in a Siemens D-500 diffractometer using  $\text{Cu}$  ( $\text{K}\alpha$ ) radiation. The simulated PXRD patterns from the single-crystal reflection data were produced using the SHELXTL 5.0-XPOW program.  $\text{N}_2$ -adsorption/desorption isotherms were obtained at a liquid  $\text{N}_2$  temperature of 77 K using a Micromeritics ASAP 2010 system, and the samples were degassed at 180 °C in a vacuum of  $10^{-5}$  Torr before measurement. The surface area and pore volume were determined using the BET method and  $t$ -plot analysis, and the average pore size was calculated on  $2V/S$ . The TGA was carried out in flowing atmosphere ( $\text{N}_2$ , flow rate = 5.0 mL/min) with a heating rate of 5 °C/min using Perkin-Elmer TAC 7/DX instruments. The elemental analyses of C, H, and N were carried out on a Perkin-Elmer 240 C, H, N elemental analyzer, and the Zn content was determined by EDTA titration.

**Synthesis of  $[\text{Zn}_3(\text{BDC})_3 \cdot (\text{H}_2\text{O})_2] \cdot 4\text{DMF}$  (**1**).** As described,<sup>12</sup> large single crystals of **1** were grown by a modified liquid–liquid diffusion of triethylamine (TEA) into a DMF solution of  $\text{Zn}(\text{NO}_3)_2 \cdot 6\text{H}_2\text{O}$  and BDC. A 15 mL DMF solution containing 0.166 g (1.0 mmol) of  $\text{H}_2\text{BDC}$  and 0.100 g (0.5 mmol) of  $\text{Zn}(\text{NO}_3)_2 \cdot 6\text{H}_2\text{O}$  was placed in a tube (dimensions of 10 mm  $\times$  150 mm). One milliliter of a DMF solution containing 2.0 mmol TEA was placed in a small vial. The vial was sealed with a stopper that had been pierced with a pinprick to allow slow emergence of the contents. This vial was then placed in the larger solution tube. The outer tube was then

- (8) For examples, see: (a) Chae, H. K.; Siberio-Perez, D. Y.; Kim, J. H.; Go, Y. B.; Eddaoudi, M.; Matzger, A. J.; O’Keeffe, M.; Yaghi, O. M. *Nature* **2004**, *427*, 523. (b) Eddaoudi, M.; Li, H.; Yaghi, O. M. *J. Am. Chem. Soc.* **2000**, *122*, 1391. (c) Kitaura, R.; Fujimoto, K.; Noro, S.; Kondo, M.; Kitagawa, S. *Angew. Chem., Int. Ed.* **2002**, *41*, 133. (d) Uemura, K.; Kitagawa, S.; Kondo, M.; Fukui, K.; Kitaura, R.; Chang, H.; Mizutani, T. *Chem.—Eur. J.* **2002**, *8*, 3586. (e) Lee, E. Y.; Suh, M. P. *Angew. Chem., Int. Ed.* **2004**, *43*, 2798. (f) Ko, J. W.; Min, K. S.; Suh, M. P. *Inorg. Chem.* **2002**, *41*, 2151. (g) Min, K. S.; Suh, M. P. *Chem.—Eur. J.* **2001**, *7*, 303. (h) Choi, H. J.; Lee, T. S.; Suh, M. P. *Angew. Chem., Int. Ed. Engl.* **1999**, *38*, 1405. (i) Min, K. S.; Suh, M. P. *J. Am. Chem. Soc.* **2000**, *122*, 6834. (j) Pan, L.; Liu, H.; Lei, X.; Huang, X.; Olson, D. H.; Turro, N. J.; Li, J. *Angew. Chem., Int. Ed.* **2003**, *42*, 542. (k) Sawaki, T.; Aoyama, Y. *J. Am. Chem. Soc.* **1999**, *121*, 4793. (l) Albrecht, M.; Lutz, M.; Spek, A. L.; van Koten, G. *Nature* **2000**, *406*, 970.
- (9) (a) Zhang, H.; Wang, X.; Zhang, K.; Teo, B. K. *Coord. Chem. Rev.* **1999**, *183*, 157. (b) Saalfrank, R. W.; Bernt, I.; Uller, E.; Hampel, F. *Angew. Chem., Int. Ed. Engl.* **1997**, *36*, 2482. (c) Cardenas, D. J.; Gavina, P.; Sauvage, J. P. *J. Am. Chem. Soc.* **1997**, *119*, 2656.
- (10) Sauvage, J. P.; Hosseini, M. W. In *Templating, Self-Assembly, and Self-Organization*; Comprehensive Supramolecular Chemistry Vol. 9; Atwood, J. L., Davies, J. E. D., Macnicol, D. D., Toda, F., Bishop, R., Ed.; Elsevier: Oxford, 1996.
- (11) (a) Baca, S. G.; Filippova, I. G.; Gerbelev, N. V.; Simonov, Y. A.; Gdaniec, M.; Timco, G. A.; Gherco, O. A.; Malaestean, Y. L. *Inorg. Chim. Acta* **2003**, *344*, 109. (b) Zheng, Y. Q.; Sun, D. J. *Solid State Chem.* **2003**, *172*, 288.
- (12) (a) Li, H.; Davis, C. E.; Groy, T. L.; Kelley, D. G.; Yaghi, O. M. *J. Am. Chem. Soc.* **1998**, *120*, 2186. (b) Edger, M.; Mitchell, R.; Slawin, A. M.; Lightfoot, P.; Wright, P. A. *Chem.—Eur. J.* **2001**, *7*, 5168.
- (13) Kitaura, R.; Seki, K.; Akiyama, G.; Kitagawa, S. *Angew. Chem., Int. Ed.* **2003**, *42*, 428.
- (14) Zeng, M.; Feng, X. Chen, X. *Dalton Trans.* **2004**, 2217.
- (15) (a) Kitaura, R.; Iwahori, F.; Matsuda, R.; Kitagawa, S.; Kubota, Y.; Takata, M.; Kobayashi T. C. *Inorg. Chem.* **2004**, *43*, 6522. (b) Prior, T. J.; Rosseinsky, M. J. *Chem. Commun.* **2001**, 495. (c) Prior, T. J.; Bradshaw, D.; Teat, S. J.; Rosseinsky, M. J. *Chem. Commun.* **2003**, 500.
- (16) Zheng, S.; Tong, M.; Fu, R.; Chen, X.; Ng, S. *Inorg. Chem.* **2001**, *40*, 3562–3569.

- (17) (a) Ohtsuka, K. *Chem. Mater.* **1997**, *9*, 2039. (b) Cheng, S.; Wang, T.-C. *Inorg. Chem.* **1989**, *28*, 1283. (c) Anderson, M. W.; Klinowski, J. *Inorg. Chem.* **1990**, *29*, 3260. (d) Pinnavaia, T. J.; Tzou, M.; Landau, S. D. *J. Am. Chem. Soc.* **1985**, *107*, 4783.

**Table 1.** Crystallographic Data for **1**, **2**, and **3**

	<b>1</b>	<b>2</b>	<b>3</b>
empirical formula	C <sub>36</sub> H <sub>44</sub> N <sub>4</sub> O <sub>18</sub> Zn <sub>3</sub>	C <sub>40</sub> H <sub>38</sub> N <sub>4</sub> O <sub>16</sub> Zn <sub>3</sub>	C <sub>47</sub> H <sub>54</sub> N <sub>4</sub> O <sub>21</sub> Zn <sub>3</sub>
fw	1016.43	1024.54	1207.1
crystal system	monoclinic	monoclinic	monoclinic
space group	<i>P</i> 2 <sub>1</sub> / <i>c</i>	<i>C</i> 2/ <i>c</i>	<i>C</i> 2/ <i>c</i>
<i>a</i> (Å)	13.045(5)	26.299(7)	33.237(12)
<i>b</i> (Å)	9.655(3)	9.998(3)	9.719(4)
<i>c</i> (Å)	18.462(6)	18, 376(5)	18.423(4)
$\beta$ (deg)	106.892(4)	123.555(3)	90.538(5)
vol (Å <sup>3</sup> )	2225.0(13)	4026.3(18)	5951(4)
<i>Z</i>	4	4	4
<i>d</i> <sub>calcd</sub> (g/cm <sup>3</sup> )	1.518	1.631	0.952
abs coeff (mm <sup>-1</sup> )	1.680	1.852	1.242
<i>F</i> (000)	5376	1944	1704
cryst size (mm)	0.6 × 0.8 × 0.8	05 × 0.7 × 0.8	0.25 × 0.2 × 0.2
$\theta$ range (deg)	1.63–26.51	1.86–25.01	2.18–27.12
limiting indices	–14 ≤ <i>h</i> ≤ 16 –7 ≤ <i>k</i> ≤ 12 20 ≤ <i>l</i> ≤ 23	–31 ≤ <i>h</i> ≤ 26 –9 ≤ <i>k</i> ≤ 11 19 ≤ <i>l</i> ≤ 21	–42 ≤ <i>h</i> ≤ 41 –12 ≤ <i>k</i> ≤ 12 –11 ≤ <i>l</i> ≤ 23
reflns collected/unique	10 275/4612 [ <i>R</i> <sub>int</sub> = 0.0373]	8092/3514 [ <i>R</i> <sub>int</sub> = 0.0369]	16 733/6517 [ <i>R</i> <sub>int</sub> = 0.0594]
data/restraints/params	4612/0/293	3514/0/288	6517/0/232
GOF on <i>F</i> <sup>2</sup>	1.033	1.010	1.026
final <i>R</i> indices [ <i>I</i> > 2σ( <i>I</i> )]	<i>R</i> 1 = 0.0344 w <i>R</i> 2 = 0.0853	<i>R</i> 1 = 0.0679 w <i>R</i> 2 = 0.1941	<i>R</i> 1 = 0.0668 w <i>R</i> 2 = 0.1787
<i>R</i> indices (all data)	<i>R</i> 1 = 0.0456 w <i>R</i> 2 = 0.0915	<i>R</i> 1 = 0.0782 w <i>R</i> 2 = 0.2040	<i>R</i> 1 = 0.0917 w <i>R</i> 2 = 0.1882
largest diff. peak and hole (e Å <sup>-3</sup> )	0.453 and –0.386	0.996 and –0.678	0.986 and –1.118

**Table 2.** Selected Bond Lengths (Å) and Angles (deg) for **1**, **2**, and **3**

		<b>1<sup>a</sup></b>			
Zn(1)–O(4)	1.9392(18)	Zn(1)–O(7)	1.940(2)	Zn(1)–O(2)	1.9654(18)
Zn(1)–O(5)	2.0080(18)	Zn(2)–O(1)	2.0325(18)	Zn(2)–O(5)	2.2013(19)
Zn(2)–O(3)	2.0698(18)				
O(4)#1–Zn(1)–O(7)	110.24(10)	O(4)#1–Zn(1)–O(2)	113.66(9)	O(7)–Zn(1)–O(2)	96.89(10)
O(4)#1–Zn(1)–O(5)	112.63(8)	O(7)–Zn(1)–O(5)	123.68(10)	O(2)–Zn(1)–O(5)	97.67(8)
O(1)–Zn(2)–O(1)#2	180.00(8)	O(1)–Zn(2)–O(3)#1	94.94(8)	O(3)#1–Zn(2)–O(3)#3	180.00(8)
O(1)–Zn(2)–O(3)#3	85.06(8)	O(1)–Zn(2)–O(5)	90.35(7)	O(1)#2–Zn(2)–O(5)	89.65(7)
O(3)#1–Zn(2)–O(5)	90.60(8)	O(3)#3–Zn(2)–O(5)	89.40(8)	O(5)#2–Zn(2)–O(5)	180.00(9)
		<b>2<sup>b</sup></b>			
Zn(1)–O(1)	2.078(4)	Zn(1)–O(8)	2.095(4)	Zn(1)–O(7)	2.127(4)
Zn(1)–O(5)	2.177(3)	Zn(1)–O(3)	2.192(4)	Zn(2)–O(2)	2.138(3)
Zn(2)–O(5)	2.249(3)	Zn(2)–O(4)	2.176(4)		
O(1)–Zn(1)–O(8)#1	118.70(16)	O(8)#1–Zn(1)–O(5)	93.86(14)	O(7)–Zn(1)–O(5)	170.43(14)
O(1)–Zn(1)–O(5)	94.40(14)	O(8)#1–Zn(1)–O(3)#2	105.63(16)	O(7)–Zn(1)–O(3)#2	81.86(15)
O(1)–Zn(1)–O(3)#2	134.38(16)	O(2)#3–Zn(2)–O(2)	180.0	O(2)–Zn(2)–O(4)#4	85.98(14)
O(5)–Zn(1)–O(3)#2	92.79(14)	O(4)#2–Zn(2)–O(5)	84.07(14)	O(2)–Zn(2)–O(5)#3	89.11(13)
O(2)–Zn(2)–O(4)#2	94.02(14)	O(2)–Zn(2)–O(5)	90.89(13)	O(4)#4–Zn(2)–O(5)	95.93(14)
O(4)#2–Zn(2)–O(4)#4	180.00(19)	O(8)#1–Zn(1)–O(7)	95.22(16)	O(5)#3–Zn(2)–O(5)	180.00(1)
O(1)–Zn(1)–O(7)	83.89(15)				
		<b>3<sup>c</sup></b>			
Zn(2)–O(1)	2.031(3)	Zn(2)–O(3)	2.051(3)	Zn(1)–O(7)	1.957(4)
Zn(1)–O(5)	1.966(3)	Zn(2)–O(5)	2.224(3)	Zn(1)–O(4)	1.986(4)
Zn(1)–O(2)	1.954(3)				
O(3)#1–Zn(2)–O(3)#3	180.0(0)	O(3)#1–Zn(2)–O(1)	95.19(15)	O(3)#3–Zn(2)–O(1)	84.81(15)
O(1)–Zn(2)–O(5)	89.84(13)	O(3)#1–Zn(2)–O(5)	90.13(13)	O(1)–Zn(2)–O(1)#2	179.997(2)
O(4)#1–Zn(1)–O(7)	106.004(18)	O(1)#2–Zn(2)–O(5)	90.17(13)	O(5)#2–Zn(1)–O(5)	179.999(1)
O(4)#1–Zn(1)–O(5)	100.09(14)	O(4)#1–Zn(1)–O(2)	111.99(16)	O(7)–Zn(1)–O(2)	96.71(17)
O(3)#3–Zn(2)–O(5)	89.87(13)	O(7)–Zn(1)–O(5)	131.99(17)	O(2)–Zn(1)–O(5)	109.87(14)

<sup>a</sup> Symmetry code: #1 *x*, –*y* + 1/2, *z* – 1/2; #2 –*x*, –*y* + 1, –*z*; #3 –*x*, *y* + 1/2, –*z* + 1/2. <sup>b</sup> Symmetry code: #1 *x*, *y* – 1, *z*; #2 *x*, –*y* + 2, *z* + 1/2; #3 –*x* + 1/2, –*y* + 3/2, –*z* + 1; #4 –*x* + 1/2, *y* – 1/2, –*z* + 1/2. <sup>c</sup> Symmetry code: #1 *x*, –*y* + 1, *z* + 1/2; #2 –*x* + 1/2, –*y* + 3/2, –*z* + 1; #3 –*x* + 1/2, *y* + 1/2, –*z* + 1/2.

sealed and left to stand at room temperature for 1 week. The colorless block-shaped crystals of **1** were obtained with a yield of 80% (based on Zn). Anal. Calcd: C, 42.48; N, 5.51; H, 4.33; O, 28.32; Zn, 19.18. Found: C, 43.36; N, 5.45; H, 4.27; Zn, 19.08.

**Synthesis of [Zn<sub>3</sub>(BDC)<sub>4</sub>]<sub>2</sub>·2HPIP (**2**).** A mixture of 1 mmol of [Zn<sub>3</sub>(BDC)<sub>3</sub>·(H<sub>2</sub>O)<sub>2</sub>]<sub>2</sub>·4DMF, **1** (1.00 g), and 0.166 g (1 mmol) of

BDC acid ligand with PIP (0.112 g, 1 mmol) in 10 mL of DMF was stirred about 30 min; then it was sealed in a Teflon-lined stainless steel bomb at 160 °C for 2 days. Finally, the colorless block crystals of **2** were obtained with a yield of 60% (based on BDC). Anal. Calcd: C, 46.79; N, 5.46; H, 3.73; O, 24.93; Zn, 19.10. Found: C, 46.90; N, 5.49; H, 3.58; Zn, 19.05.



**Synthesis of  $[\text{Zn}_3(\mu\text{-BDC})_3(\text{H}_2\text{BDC})] \cdot (\text{C}_6\text{H}_5\text{NO}) \cdot (\text{H}_2\text{O}) \cdot 3\text{DMF}$  (**3**).** The procedure was similar to that used for **2**. One millimol of  $[\text{Zn}_3(\text{BDC})_3 \cdot (\text{H}_2\text{O})_2] \cdot 4\text{DMF}$  (1.00 g), 0.166 g (1 mmol) of BDC ligand, and 0.112 g (2 mmol) of TEA were mixed in 20 mL of acetic acid/DMF ( $v/v = 1/3$ ) for about 30 min; then the mixture was sealed in a Teflon-lined stainless steel bomb at 160 °C for 3 days. Finally, the colorless block crystals of **3** were obtained (yield 85%, based on BDC). Anal. Calcd: C, 46.77; N, 4.64; H, 4.51; O, 27.83; Zn, 16.25. Found: C, 46.65; N, 4.72; H, 4.47; O, 27.75; Zn, 16.38.

**X-ray Crystallography.** A full hemisphere of data for **1**, **2**, and **3** was collected on a Bruker SMART Apex CCD diffractometer with Mo  $K\alpha$  radiation ( $\lambda = 0.71073 \text{ \AA}$ ) at 293 K. The frames were integrated with the SAINT software package.<sup>25</sup> The structure was solved by direct methods, and the subsequent difference Fourier synthesis was refined with the SHELXTL, version 5.10, software package.<sup>25</sup> The refinement was done with full-matrix least-squares method on  $F^2$ . The non-hydrogen atoms were refined with anisotropic thermal parameters, except the disorder guests in **3** were included. No H atoms associated with the water molecules of **1** and **3** were located in the difference Fourier maps, and the hydrogen atoms were included in the refinement in calculated positions riding on their carrier atoms. The hydrogen atoms were refined with a fixed isotropic displacement parameter related to the value of the equivalent isotropic displacement parameter of their carrier atoms. The contribution to the structure factors associated with the disorder guests in **3** were taken into account using the SQUEEZE procedure as incorporated in PLATON.<sup>26</sup> Additional details are provided in Tables 1 and 2.

## Results and Discussion

**Synthesis.** Compound **1** can be easily prepared by the modified liquid–liquid diffusion in an 80% yield.<sup>12</sup> The structure analysis shows that **1** has a layered structure with some sites occupied by some labile  $\text{H}_2\text{O}$  molecules. Further reaction of **1** with BDC as shown in Scheme 1, produced two 3D layer-pillared compounds, **2** and **3**. In the solvo-thermal process to form **2** and **3**, the same solvent was employed as in the preparation of **1**, but different organic amines were used as bases to remove protons from the BDC ligand. These amines were *n*-butylamine (BA), di-*n*-butylamine (DBA), diisopropylamine (*i*-DPA), TEA, phenylamine (PHA), PIP, cyclohexylamine (CHA), 1,4-diazobicyclooctane (DABCO), and hexamethylenetetraamine (HMTA). The best yield of **2** (60%) was obtained with PIP in equimolar proportions to BDC. The yields of **3** were unacceptably low with all amines. Attempts to improve the yield of **3** by adjusting the molar ratio of reactants (in proportion to **1**) in the ranges, BDC 1–5, TEA 0.1–4, and DMF 10–1000 at 100–180 °C were unsuccessful.

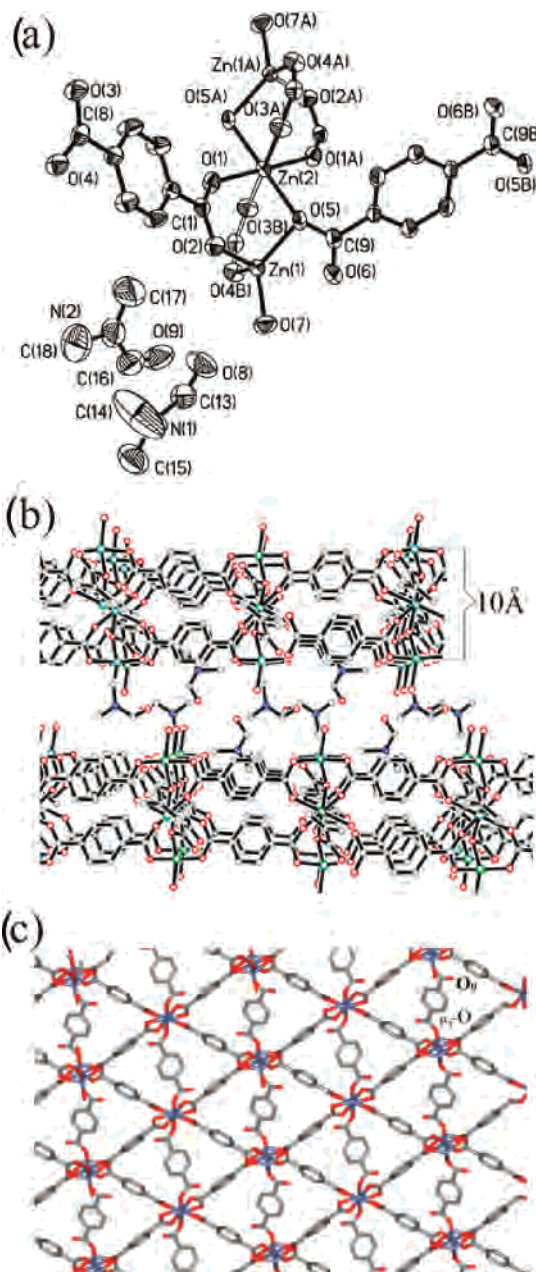


**Figure 1.** Crystal structure of **1**: (a) the coordination environment of the  $\text{Zn}_3$  cluster, (b) the stacking diagram of layered structure, and (c) the monolayered structure.

The effect of acids in the reaction system on the yield of **3** was investigated with  $\text{HNO}_3$ ,  $\text{HCl}$ ,  $\text{HAc}$ , and  $\text{HCOOH}$  in a reaction mixture of molar proportions of  $1/\text{BDC}/\text{TEA}/\text{DMF} = 1:1:2:15$ . It was found that  $\text{HAc}$  was the most successful in improving the yield of **3** at 160 °C. Furthermore, when the volume ratio of  $\text{HAc}/\text{DMF}$  was adjusted to 1:3, the yield of **3** improved to 85%. This may be explained if  $\text{HAc}$ , the weakest acid of the trial set, forms a buffer pair with TEA so that the acidity change is minimized in optimal proportions. The role of organic amines in facilitating the assembly of carboxylate-based coordination polymers by proton removal is already recognized.<sup>27</sup> However, as only PIP and TEA result in **2** and **3**, respectively, this suggests that PIP and TEA are not only acting as organic bases but also play a role in directing structure during the assembly of the

(18) Seki, K.; Mori, W. *J. Phys. Chem. B* **2002**, *106*, 1380.

(19) Seki, K. *Chem. Commun.* **2001**, 1496.

(20) Dybtssev, D. N.; Chun, H.; Kim, K. *Angew. Chem., Int. Ed.* **2004**, *43*, 5033.

(21) Choi, E. Y.; Park, K.; Yang, C. M.; Kim, H.; Son, J. H.; Lee, S. W.; Lee, Y. H.; Min, D.; Kwon, Y. U. *Chem.—Eur. J.* **2004**, *10*, 5535.

(22) Choi, H. J.; Suh, M. P. *J. Am. Chem. Soc.* **2004**, *126*, 15844.

(23) Kitaura, R.; Fujimoto, K.; Noro, S.; Kondo, M.; Kitagawa, S. *Angew. Chem., Int. Ed.* **2002**, *41*, 133.

(24) Uemura, K.; Kitagawa, S.; Kondo, M.; Fukui, K.; Kitaura, R.; Chang, H.; Mizutani, T. *Chem.—Eur. J.* **2002**, *8*, 3586.

(25) *SHELXTL*, version 5.10; Bruker Analytical X-ray: Madison, WI, 1997. (b) *Saint Software Package*, version 6.01; Bruker Analytical X-ray: Madison, WI, 1999.

(26) Van der Sluis, P.; Spek, A. L. *Acta Crystallogr.* **1990**, *A46*, 194.

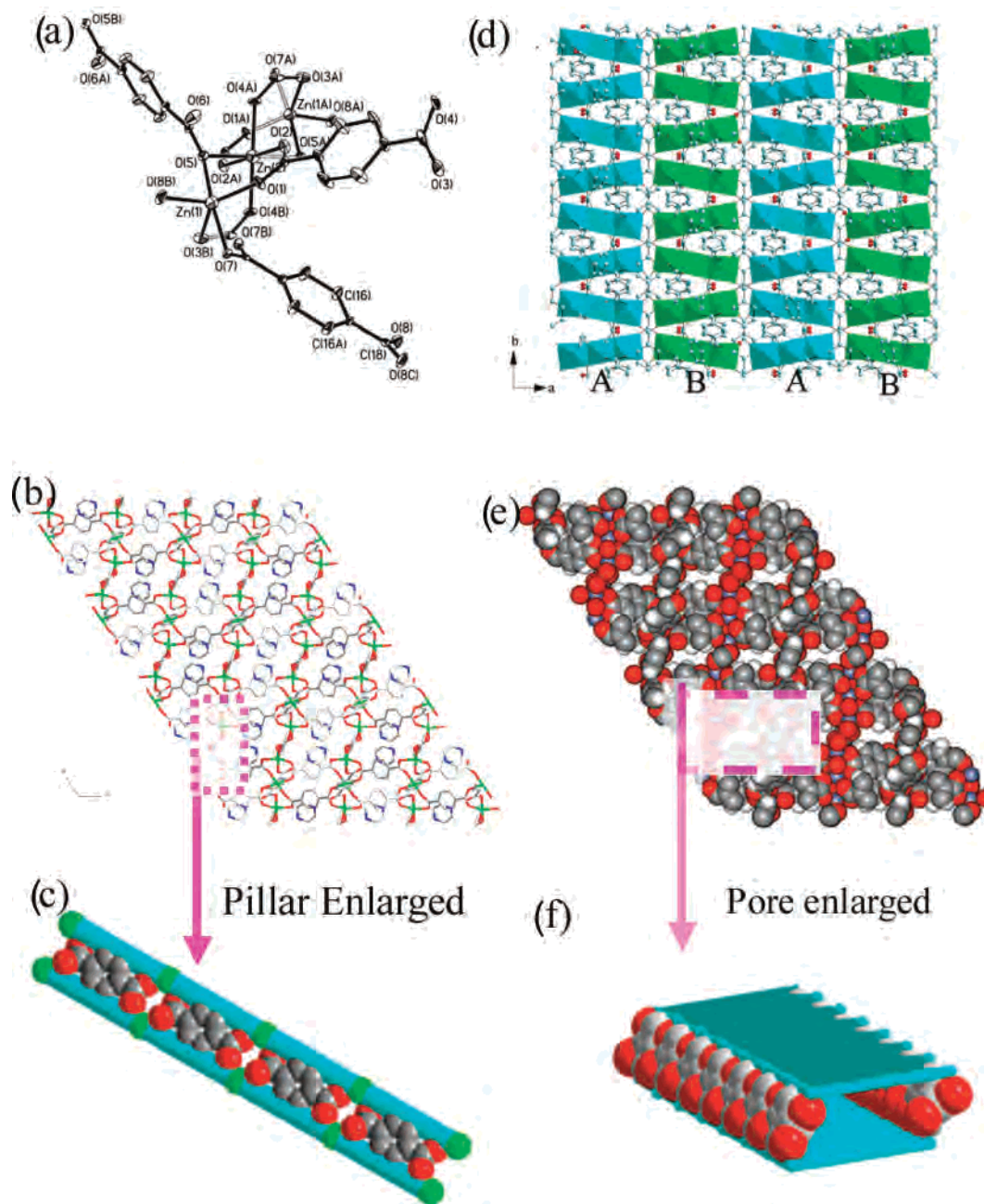


**Figure 2.** Crystal structure of **2**: (a) the coordination environment of the  $Zn_3$  cluster, (b) the channel structure with PIP guest molecules, (c) the local enlarged section of pillars showing their linkage to the  $Zn_3$  cluster (green sphere is  $Zn(II)$ ) and the array of interpillars, (d) the stacking sequence of the layer structure, (e) a CPK diagram representing the open framework, and (f) the enlarged section of its channels.

coordination polymer. This role has been observed in the synthesis of inorganic molecular sieves.<sup>28,29</sup>

To estimate the effect of the layered precursor on **2** and **3**, compound **1** was replaced by a mixture of equimolar zinc nitrate (or  $ZnAc$ ) and BDC acid. It was found that **2** can also be prepared by using zinc salts and BDC ligands as starting materials in the presence of PIP, but **3** was not formed. However, **3** can be obtained directly from **1** in its mother liquid with BDC. So it is concluded that the formation

of **3** depends on the presence of **1**. This suggests that the formation of **2** and **3** follow different mechanisms.

**Structure.** SCXRD (Figure 1) shows that **1** is a 2D layered structure. It possesses a  $Zn_3$  cluster unit in which two tetrahedral  $Zn(1)$  atoms sandwich an octahedral  $Zn(2)$  core as reported for  $[Zn_3(BDC)_3(H_2O)_2] \cdot 4DMF$ <sup>12b</sup> but different from MOF-3.<sup>12a</sup> Its  $Zn(1)$  binding to a terminal water ligand displays tetrahedral geometry, while the counterpart of MOF-3 binding to two terminal methanol molecules displays bipyramidal geometry.

Figure 2 shows that **2** is a layer-pillared 3D structure. The framework in **2** is made up of a trinuclear  $Zn_3$  cluster unit with a sandwiched structure (Figure 2a); the units are bridged by two crystallographically nonequivalent BDC anions to

(27) Yaghi, O. M.; Davis, C. E.; Li, G.; Li, H. *J. Am. Chem. Soc.* **1997**, *119*, 2861.

(28) Flanigen, E. M.; Patton, R. L.; Wilson, S. T. *Stud. Surf. Sci. Catal.* **1998**, *37*, 13.

(29) Arharcet, J. P.; Davis, M. E.; Bromice, J. *Chem. Mater.* **1991**, *3*, 567.



form a triangle-tessellated layered structure, as shown in Figure 1c. The other two coordination sites of Zn(1) in this sandwich structure are occupied by O(7) and O(8) of the two independent BDC anions, respectively, which act as pillars to extend the 2D sheet into a 3D structure as shown in model **III** in Scheme 1 (Figure 2b and d). Although the bipyramid geometry of the five-coordinate Zn(1) in **2** is different from the tetrahedral one of Zn(1) in **1**, compound **2** may be viewed as a product of **1** pillared by a third crystallographically nonequivalent BDC ligand. Each BDC pillar in **2** is completely deprotonated to link four Zn<sub>3</sub> clusters together through four oxygen atoms of two carboxyl groups (Figure 2c), standing laterally between the neighbor layers with an angle of nearly zero of its long molecular axis with the Zn(2) plane in one layer (Figure S2). Since the BDC pillars arrange in an end-to-end manner (Figure 2c), **2** only exhibits a 1D channel with rather narrow slit-window of  $4.8 \times 1.2 \text{ \AA}$  in **2** (Figure 2e, 2f). However, its pore volume of  $0.205 \text{ cm}^3/\text{g}$  (28.8% of unit cell volume) can be calculated by PLATON.<sup>26</sup> Such a pore can accommodate two monoprotonated HPIPs guests as shown in Figure 2b. These guests are linked to the uncoordinated oxygen atoms of O(6) in the layer of **2** via a hydrogen bond, the length of which ( $\text{O}(6) \cdots \text{N}(1)$ ) is  $2.741 \text{ \AA}$ . This structural information showed that PIP acts as a template in **2**. All the layers are arranged in an ABAB stacking manner in the crystal lattice of **2** (Figure 2d), which is shifted  $a + b/2$  relative to its neighbors.

Figure 3 shows that **3** has the open 3D framework with 2D intersected channels. Figure 3a further shows that one trinuclear Zn<sub>3</sub> unit remains in **3**. This cluster is linked by two kinds of BDC anions into the same layer as **1** and **2** (Figures 1c and S3). This layered structure is extended into a layer-pillared 3D structure, **3**, by Zn(1) coordinating to O(7) of a third crystallographically nonequivalent H<sub>2</sub>BDC (Figure 3b and c). As a pillar, this BDC ligand is not deprotonated so that it only can link two Zn<sub>3</sub> clusters together through the carboxyl group, which stands vertically in the interlayer, such that the angle of its long axis with the plane of the Zn(2) layer is  $94.2^\circ$  (Figures 3b and S4). This structure agrees well with model **II**, expected in Scheme 1, and exhibits an intersected 2D channel with pore sizes of  $6.7 \times 4$  and  $6.5 \times 4.3 \text{ \AA}$ . In this structure, we do not find a TEA molecule, but a disorder guest molecule of TEA oxide with a water molecule and three DMFs is observed in the 2D channel. TEA oxide may be the product of TEA oxidized by molecular oxygen in the solvothermal condition of high temperature. This was confirmed by ESR spectra. These layers are also arranged in an ABAB stacking fashion (Figure 3c), which is shifted  $a - b/2$  relative to its neighbors.

Compared to its precursor **1**, compound **2** has a significant change in the geometry of Zn(1), transforming it from tetrahedral coordination to a bipyramidal form. However, **3** retains the tetrahedral geometry of **1**. This difference in the geometry of Zn(1) between **2** and **3** is consistent with the finding that **1** is a necessary precursor for **3** but is not necessary for **2**.

**Hypothesis.** It is proposed that the formation of **2** follows the process of Ostwald ripening.<sup>30</sup> This principle conceives

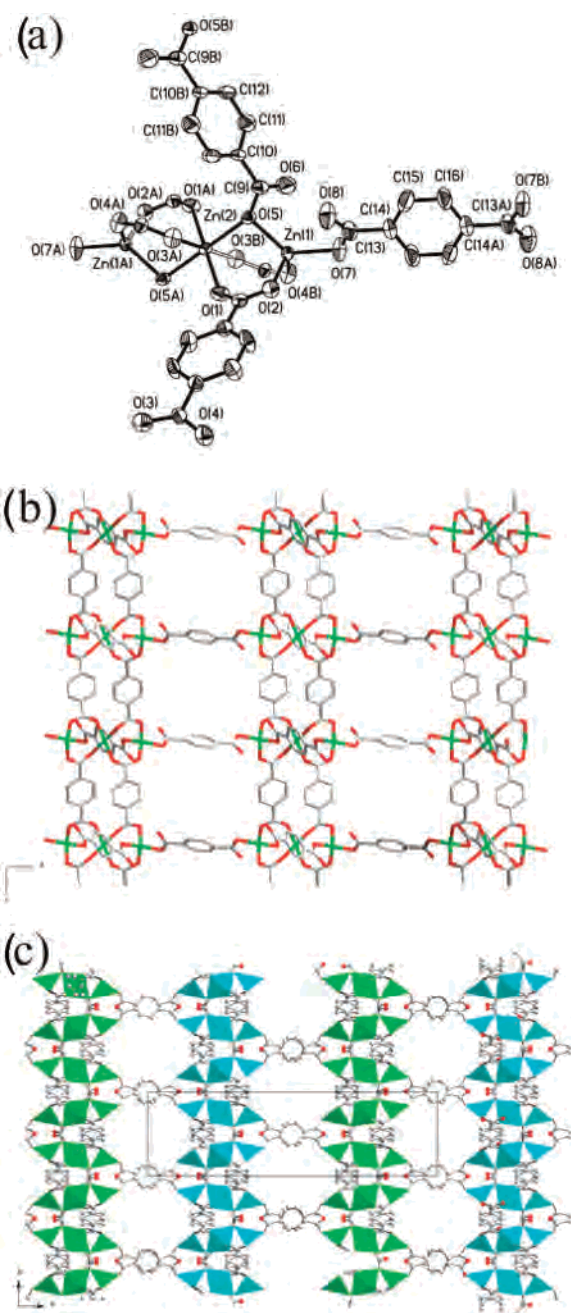


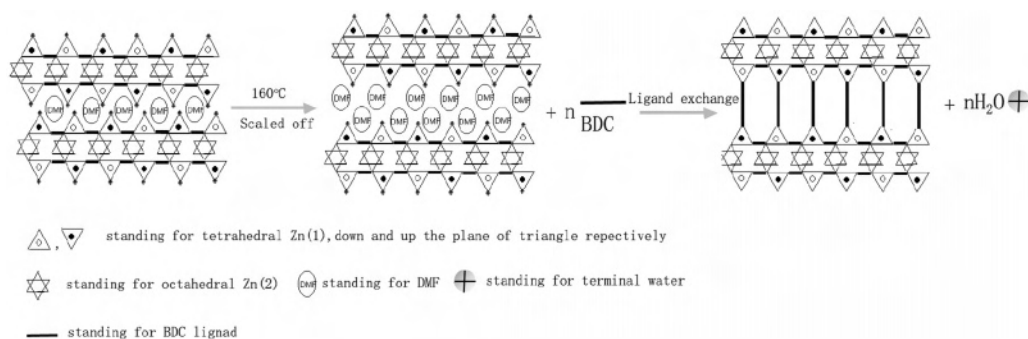
**Figure 3.** Crystal structure of **3**: (a) the coordination environment of Zn<sub>3</sub> cluster, (b) one channel of  $6.7 \times 4 \text{ \AA}$  and a pillar joining to two Zn<sub>3</sub> clusters, and (c) the stacking sequence of the layer, showing another channel of  $6.5 \times 4.3 \text{ \AA}$ .

that crystal growth is by processes of atom-to-atom addition onto a template or by dissolution of unstable phases and reprecipitation of a more stable phase.<sup>30</sup> With application of this concept, **1** can be viewed as an unstable phase that is dissociated then reassembled in the presence of PIP to form **2**. Furthermore, **2** is a PIP-induced stable phase, which may be derived from **1** or a zinc salt and BDC. In addition, the role of PIP is as a template, as observed in inorganic molecular sieve studies.<sup>28,29</sup>

It is proposed that the formation of **3** follows a different mechanism, as shown in Scheme 2. Compound **1** is first

(30) Banfield, J. F.; Welch, S. A.; Zhang, H.; Ebert, T. T.; Penn, R. L. *Science* **2000**, *289*, 751.

Scheme 2 Possible Mechanism for the Formation of 3



modified into some layered intermediates, and then BDC ligands are inserted into two neighboring layered structures, finally a 3D layer-pillared framework is reassembled. The overall result is that each new BDC in the product exchanges with two terminal waters in the starting material. This hypothesis accounts for the finding that **1** is required for the synthesis of **3** and also explains how Zn(1) retains its tetrahedral geometry in **3**.

**Physical Properties.** The TGA of **1** shows that it loses four DMFs and one coordinated water molecule below 250 °C (found 30.6%, calcd 30.5%), but until 330 °C, its

framework is not decomposed. The TGA of **2** shows a two-step weight loss in the range of 200–400 °C. The first, corresponding to a loss of ~25% appears in the range of 200–300 °C. It is proposed that this corresponds to the loss of two PIP molecules and the decarboxylation of a BDC ligand molecule (theoretical loss = 25.66%). This shows that when the guest molecule PIPs are removed, the framework collapses with the simultaneous loss of two carbon dioxide molecules. The XRD patterns and N<sub>2</sub> sorption further support this conclusion (Figures S5 and S6). The thermal stability of **3** analyzed by the TGA is shown in Figure S7. A three-step weight loss occurs. At 50–100 °C, one guest water molecule is lost (about 1.7%, calcd 1.66%); at 100–150 °C, one TEA oxide molecule and three DMF molecules are lost (up to 28.01%, calcd 27.93%), and at 300–400 °C, the decomposition of the structural framework to leave a residue of ZnO occurs (about 49.46%, calcd 50.49%). The overall process for **3** shows that occluded guest molecules in pore channels are lost at lower temperatures, while the structural framework is stable up to 300 °C.

Figure 4 shows that the PXRD pattern of **3** calcined at 180 °C under vacuum agrees with the simulated one. This suggests that the structure is thermally stable after the guest molecules in its channels are removed. The N<sub>2</sub>-adsorption/desorption isotherms (Figure 5) show a typical type I curve including a plateau reached at low relative pressure. This is characteristic of sorption in micropores. The calcined **3** samples have a relatively high BET surface area of 750 m<sup>2</sup>/g and a pore volume of 0.36 cm<sup>3</sup>/g. On the basis of the isotherm, the microporous surface area of **3** is calculated by the *t*-plot method to be 705 m<sup>2</sup>/g, suggesting that the porosity is mainly contributed by its micropores. The calculated average pore size,  $2V/S^{3/2}$  (*S* is the Langmuir surface area of 1080 m<sup>2</sup>/g), is close to the observed size of 6.5 Å.

## Conclusion

In summary, we have successfully prepared two 3D layer-pillared homoligand coordination polymers **2** and **3** starting from a layered precursor **1**. Compound **2** holds a 1D slit channel in which there are two HPIPs, while **3** has a intersected 2D channel in which there is one water guest, one oxidized TEA, and three DMFs. These guest molecules

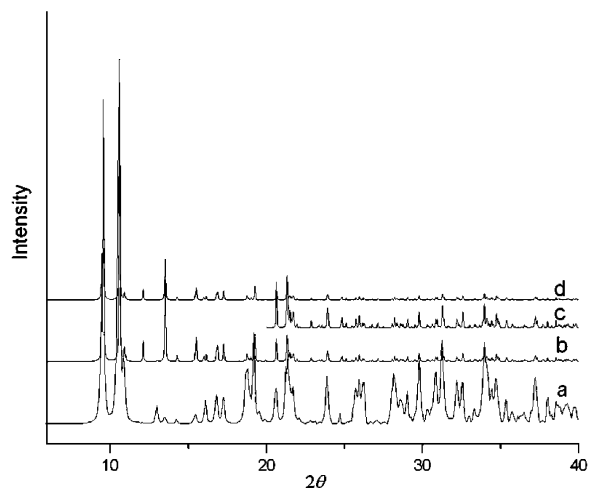


Figure 4. XRD pattern of **3**: (a) simulated from single-crystal data, (b) as-synthesized samples, (c) the scale drawing  $\times 5$  of the b plot in the  $\theta$  range of 20–40°, and (d) the calcined samples at 180 °C.

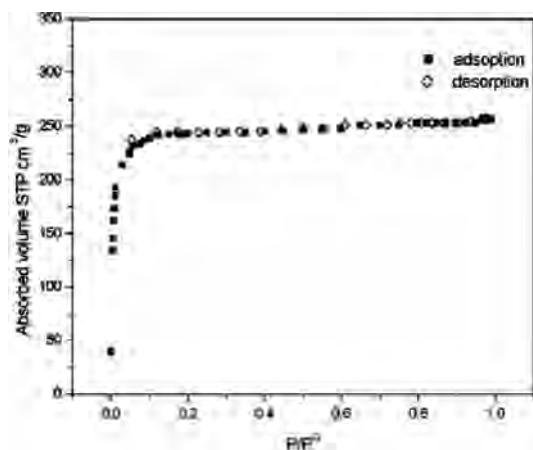


Figure 5. N<sub>2</sub>-adsorption/desorption isotherms of **3**.

(31) The average pore is calculated on three models including slit-shaped pore ( $2V/S$ ), cylindrical pore ( $4V/S$ ), and spherical pores ( $6V/S$ ). Among them, the calcd value on the slit-shaped model is nearest to the observed.

of **3** can be released at 180 °C under vacuum. Compound **3** exhibits a high BET surface area of 750 m<sup>2</sup>/g and a pore volume of 0.36 cm<sup>3</sup>/g. It is proposed that the growth of **2** is described by the Ostwald ripening principle, whereas the formation of **3** involves an insertion mechanism.

**Acknowledgment.** We thank to the NSF of China (29925309 to D.Z., 20101004 to S.Q.), the State Basic Research Project (G2000077507 to S.Q., G200048001 to D.Z.), the Chinese Ministry of Education and the Postdoctoral Fellowship of China (Grant 20040350169 to J.S.) for

financial support. We especially thank Canadian linguist Nanette Venema from Lambton College, Jilin University, and Chemist Dr A. W. Jackson of Brampton, Ontario, Canada, for the editing assistance in the preparation of this paper.

**Supporting Information Available:** Extensive figures, analytical and spectral characterization data, and crystallographic information files (CIF) of **1**, **2**, and **3**. This material is available free of charge via the Internet at <http://pubs.acs.org>.

IC0612303